Kinetics of Coil Overlap in Ionomer Blends by ^{1}H NMR in DMSO-d_6. 2. Mechanistic Aspects

F. Bossé and A. Eisenberg*

Department of Chemistry, McGill University, 801 Sherbrooke Street West, Montréal, Québec, Canada H3A 2K6

Received July 8, 1993; Revised Manuscript Received January 12, 1994®

ABSTRACT: ^{1}H nuclear magnetic resonance (NMR) studies were carried out on solutions of blends of lightly sulfonated polystyrenes (PS–SSA; 5–15 mol % sulfonation) of molecular weight (MW) 12 000 and 100 000, with poly(methyl methacrylate-*co*-4-vinylpyridine) (PMMA–4VP) copolymers (11 mol %) of MW ≅ 100 000. The process of coil overlap was monitored as a function of time by the acquisition of proton spectra, which showed the gradual disappearance of the original methoxy signal and the appearance of a new signal originating from the shielded methoxy protons. The contributions of the two species were separated using a deconvolution program. To propose a complete model for the coil overlap phenomenon, parameters that can influence the kinetics of the process were studied. The parameters included the ion content and the MW of the PS-SSA, the temperature, and the total polymer concentration. The study of these parameters showed that the overlap was occurring through a complex mechanism. It was determined that the *true order* (n_c) for the shielding process was second-order, reflecting the early stages of the mixing process. At the stage at which a "ladder"-like complex is produced, the experimental data can best be represented by a kinetic expression containing two opposing first-order reactions.

1. Introduction

Physical blending of polymers offers a route to improve polymer properties, and the area has been the subject of increasing interest over the last few decades.[1-7] However, for thermodynamic reasons, most polymer pairs are not miscible and blends formed from such pairs tend to phase separate. The lack of strong cohesive forces between the phases in such blends gives rise to poor mechanical properties, which greatly limits the number of industrial applications of these materials. Therefore, since the entropy of mixing of polymers is very low, mixing is enthalpy-driven and favorable interactions are needed for a polymer pair to be compatible. One method to obtain such favorable interactions consists of introducing the appropriate ionic groups onto each polymer chain.[8]

Many techniques can be used to determine the extent of phase separation in polymer blends. However, in order to achieve an in-depth understanding of the parameters influencing miscibility, both the individual polymers and the resulting blend must be studied down to a molecular level, and this is feasible using any of three spectroscopic techniques, i.e., IR,[9] NMR,[10] and fluorescence.[11]

In a previous study by Natansohn and Eisenberg, ^{1}H NMR spectroscopy was used to probe the miscibility of a blend of poly(methyl methacrylate-*co*-4-vinylpyridine) (PMMA–4VP) with poly(styrene-*co*-styrenesulfonic acid) (PS–SSA) in a DMSO solution.[12] This technique was useful because the methoxy proton signal of MMA is very sensitive to aromatic shielding effects, in this particular case due to the aromatic rings of the styrene units. It was previously demonstrated[13] that proton transfer from the SSA group to the pyridine ring takes place very rapidly; by contrast, it was found[12] that mixing of the two types of polymers is a slow process dictated by segmental motion in solution.

In that paper, Natansohn and Eisenberg suggest that the blending process occurring between PS–SSA and PMMA–4VP is due to proton transfer that occurs between SSA and 4VP, which, in turn, generates the oppositely charged ions which are the driving force responsible for the miscibility of PS–SSA and PMMA–4VP. It was proposed that the formation of these ion pairs brings the two chains close to one another.

The electrostatic nature of the coil overlap process was confirmed by a subsequent paper by Bossé and Eisenberg.[14] In that paper, it was shown that microelectrolyte concentrations on the order of the polymer ion content in solution could completely disrupt the interaction; trace quantities of electrolytes, by contrast, did not affect the process. It was also shown that the water content of the DMSO-d_6 solutions did not have a significant effect on the Coulombic interaction or on the overall shielding process. Experiments describing the influence of the MW, the SSA and 4VP contents, and the temperature on the Coulombic interaction were also described in that paper. These experiments determined that the electrostatic interaction was still present at relatively high temperatures, even though no shielded methoxy peak could be observed. The experiments clearly demonstrated that the electrostatic interaction has a major role to play in all phases of the coil overlap process.

In the previous studies,[12,14] it was demonstrated that intimate blending occurs in DMSO solution. However, the detailed mechanism and the parameters influencing the coil overlap or interpenetration remained unknown. To explore this aspect, the ^{1}H NMR aromatic shielding phenomenon can be used to perform quantitative kinetic experiments, the parameters being the total polymer concentration, the SSA content, the molecular weight, and the temperature.

The subject of chemical kinetics is concerned with the quantitative study of the rates of chemical reactions and the factors on which they depend. Historically, most of the studies involving kinetics of proton-transfer reactions have been performed on two types of systems, i.e., on systems containing two low molecular weight materials in aqueous solutions or one low molecular weight compound with a polymeric chain.[15] However, little information is available on the kinetics of proton transfer in systems composed of two polymer chains.[16,17] The paper by Bakeev et al.[18] is, to our knowledge, the only comprehensive study that deals with kinetics of coil overlap. These workers

* Author to whom correspondence should be addressed.
® Abstract published in *Advance ACS Abstracts*, March 15, 1994.

0024-9297/94/2227-2853$04.50/0

Table 1. Summary of the Characteristics of the PS–SSA Copolymers

MW	polydispersity index for the PS	SSA content (%)	mean no. of SSA units per chain
10^4	1.10	5.3	6
		8.3	10
		9.2	11
		10.5	12
		13.8	16
10^5	1.07	7.7	74
		10.0	96
		14.7	141

used the method of fluorescence quenching to study the formation of polyelectrolyte complexes and their ability to participate in interpolyelectrolyte reactions. The study was performed in a buffered aqueous solution, using two water-soluble polymer chains of relatively low MW, i.e., sodium poly(methacrylate) (PMANa) and poly(*N*-ethyl-4-vinylpyridinium) bromide (PEVPB). First, they form the [PMANa–PEVPB] complex, and then they perform an exchange reaction between tagged PMANa chains and those involved in the complex. They found that the reaction mechanism follows a simple second-order scheme and that the reaction is irreversible due to the presence of additional selective nonelectrostatic interactions between the polycation and polyanion chains. For this system, they found that the rate constant of the exchange reaction is independent of the polyanion chain length and increases sharply with decreasing polycation chain length, or decreasing ion content, and increasing ionic strength of the water–salt solution. However, that study is quite different from the one described in this paper. First, the study was performed in a different solvent (bidistilled water), with two water-soluble polymer chains of relatively low MW. Second, the exchange reaction is irreversible. As will be seen, this mechanism is quite different for the global coil overlap process. Thus, the purpose of the present investigation is to explore the kinetics of the coil overlap process in detail, over a wide range of experimental parameters.

2. Experimental Section

2.1. Synthesis and Characterization of the Copolymers. The PMMA–4VP copolymer of 11 mol % VP was synthesized as part of another project.[19] This polymer was prepared by radical bulk copolymerization and was found to have a viscosity-average molecular weight (M_v) of 10^5. Using established procedures, the VP content was determined by nonaqueous titration.[20] The molecular weight of the PS samples (Polyscience) was determined by size-exclusion chromatography, using a Varian 5000 LC apparatus. The solvent was tetrahydrofuran at 25 °C, and the standardization involved five "monodisperse" PS reference samples (Varian TSK kit). Analyses were performed in duplicate, with the number of repeat units determined to a precision of about 5%. The polydispersity index was found to be 1.1. The acid copolymers based on monodisperse PS were synthesized according to an established procedure suggested by the patent of Makowski et al.[21] This procedure was used to sulfonate monodisperse polystyrene samples with molecular weights of 12 000 and 100 000. The extent of sulfonation was varied between 5 and 15 mol % of SSA units. The titration procedure for the determination of the sulfonic acid content in the copolymers is described elsewhere.[22] The PS–SSA titrations were performed in triplicate, and the average deviation in the SSA content was less than 1%. These results are summarized in Table 1.

2.2. Blending. Solutions of the blends were prepared using the following procedure: Equimolar quantities of the two dried copolymers were weighed separately to a total of 10 mg. The PMMA–4VP was then placed in a predried NMR tube and the PS–SSA in a predried vial. Subsequently, 0.25 mL of DMSO-d_6 was added to each copolymer. Both copolymer solutions were then placed for 15 min in a thermostated bath set at the experimental temperature. Subsequently, the PSS–SSA solution was injected with a syringe into the NMR tube containing the PMMA–4VP solution, and the NMR tube was immediately placed in the probe at the experimental temperature. It is important to note that the 4VP content and the molecular weight of the PMMA–4VP were kept constant for all the blends investigated in the present study, i.e., a VP content of 11 mol % and a MW of 10^5. Moreover, the term blend that will be used throughout this paper refers to mixtures in solution and must not be confused with blends in the solid state.

All NMR spectra were acquired in a DMSO-d_6 solution using a Varian XL-300 spectrometer. The deuterated DMSO (Aldrich; 99.96% deuterated) was used as received. The pulse sequence employed was a standard S2PUL with 32 transients. In order to minimize the acquisition time, ^{1}H NMR spectra were monitored for the spectral range included between 4.0 and 3.0 ppm. The pulse sequence employed was a standard S2PUL with 16 transients. The S2PUL sequence consists of a 90° pulse with a width of 11 μs, followed by an acquisition time of 2.51 ms. The free induction decays (FIDs) were accumulated via 512 time-domain data points, with a pulse repetition delay of 1.5 s. Since the proton spin–lattice relaxation times for both polymers in the laboratory frame are much less than 1 s, this ensures that the proton spectra are fully relaxed, and no signal distortion should be expected.

2.3. Deconvolution Process. The deconvolution process involves the separation of a complex curve into a certain number of independent contributions, which, when added to the proper base line, will reconstruct the original line shape. The procedure used to achieve the deconvolution of the superposed ^{1}H NMR signal of the two methoxy groups was described elsewhere.[23]

The deconvolution of the NMR spectral line shapes was performed by a FORTRAN program developed in this group. The deconvolution program had to be developed, since at that time (≅1985) no commercial packages were available. The documented FORTRAN listing for this program can be found in ref 23. This program performs a step-size nonlinear least-squares estimation of a combination of two common idealized band shapes, Lorentzian and/or Gaussian, using a modified algorithm developed originally by Marquardt.[24] An algebraic expression modeling those two distributions is obtainable using three standard nonlinear parameters i.e., the height for the intensity maximum, the width at half-height, and the position of the maximum of the band.

The algorithm does an iterative minimization of the intensity function using a steepest-descent procedure. As suggested in ref 25, a step-size parameter is used in order to avoid pitfall caused by the presence of local minima in the function. The process usually converged rapidly, i.e., in less than 10 iterations. The selected convergence criterion for the experimental spectrum is the χ^2 test, which is a standard procedure to verify the adjustment of a series of experimental observations to a given statistical model. For all the deconvoluted line shapes, the confidence level is 95% and the value of the correlation coefficient is always close to 1 (>0.995), which indicates an excellent correlation between the experimental and the deconvoluted line shape.

2.4. Line Shape of the Signal due to the PMMA–4VP Methoxy Groups. Before one can attempt qualitative or quantitative kinetics studies, it is necessary to explore and define the real line shape of the methoxy group in pure PMMA–4VP in the absence of the PS–SSA. Moreover, since the experiments are carried out over a relatively wide range of temperatures, it is crucial to know the influence of the temperature on the methoxy group line shape. This was achieved by the acquisition of ^{1}H spectra of the pure PMMA–4VP (5 mg/0.5 mL of DMSO-d_6) over a temperature range from 60 to 120 °C in increments of 5 °C. From Figure 1, one can see that the line shape of the pure PMMA–4VP methoxy groups at 120 °C is not due to a single band but is composed of several such bands. The individual features of the main methoxy signals that appear in the range of 3.62–3.48 ppm were assigned to methoxy groups in MMA sequences and to those in cosyndiotactic MMA–4VP sequences in terms of pentads.[26] Thus, this signal is composed of features due to the following sequences: 11111, 21111, 12111, 22111, 21112, 12121, and 21212, where the indices 1 and 2 refer respectively to the MMA and 4VP units. At 120 °C, these seven independent

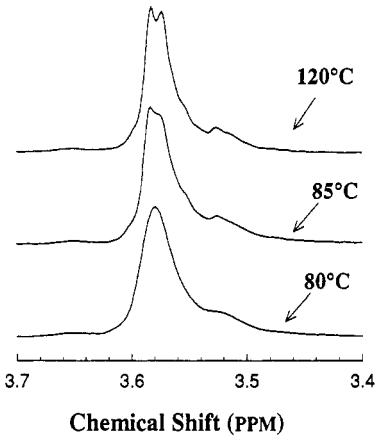

Figure 1. ^{1}H NMR spectra for the methoxy groups from PMMA–4VP at various temperatures.

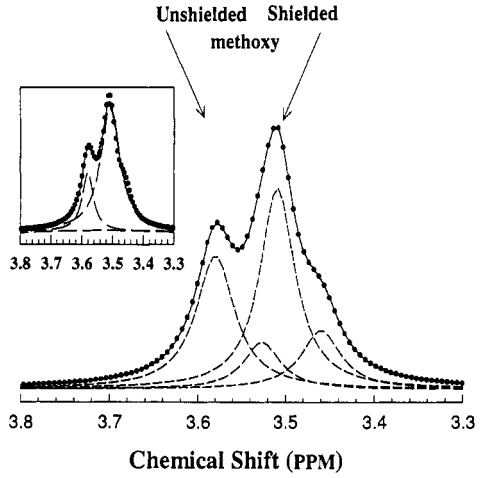

Figure 2. ^{1}H NMR spectra for the methoxy groups for a blend of PS–SSA (10 mol %) of MW = 10^4 with PMMA–4VP at 85 °C (contact time = 30 min). Resolution into four Lorentzian peaks is shown. The inset contains an illustration of the procedure involving resolution into two Lorentzian peaks.

contributions can be assigned to the following bands: the shoulder observable at ≅3.61 ppm is due to the 11111 sequences, the two main peaks at 3.59 and 3.57 ppm are due to the 21111 and 12111 sequences, respectively, and the shoulder at ≅3.55 ppm is due to the 22111 sequences, while the broad signal centered around 3.52 ppm results from a combination of the three remaining sequences (21112, 12121, and 21212). These assignments were made on the basis of the relative induced shielding from the 4VP nitrogen atoms on the PMMA methoxy groups, as discussed by Natansohn, Maxim, and Feldman.[26]

For temperatures lower than 120 °C, the two main bands attributed to the 21111 and 12111 sequences coalesce. Furthermore, at 85 °C the two previous signals that appear at 3.59 and 3.57 ppm almost form one band, and only one featureless signal is observable for the two sequences. Empirically, it was found that, for temperatures higher than 85 °C, the methoxy group line shape can be approximated using three Lorentzian bands, while for spectra taken below that temperature only two Lorentzian bands are required. For temperatures >85 °C, this procedure neglects the two shoulders attributed to the 11111 and 22111 sequences and only three bands, i.e., the two sharp signals attributed to the 21111 and 12111 sequences and the shoulder that is the combination of three sequences (21112, 12121 and 21212). For temperatures under 85 °C, we also neglect the two shoulders (11111 and 22111) and assume that 21111 and 12111 can be fitted by only one Lorentzian band. The validity of this approach was verified by the deconvolution of the methoxy group line shape obtained for each temperature; an excellent correlation (>0.995) between the experimental spectrum and the fitted line shape was obtained. From this fact it can be concluded that the contribution to the total line shape of the two shoulders due to the 11111 and 22111 sequences can be neglected and that a minimum number of bands (2 or 3) could satisfactorily duplicate the experimental line shape of the methoxy groups.

Deconvolution of the methoxy group line shapes indicates that the contributions of each of the methoxy bands to the total area are temperature independent, which is reasonable, since they are due to the sequences included in the polymer chain. Thus, one can calculate the mean percent area of the shoulder to the total area of the homopolymer methoxy signal as a function of temperature, which was found to be 27.3 ± 1.2. Obtaining the relative area contribution of the shoulder to the total area of the homopolymer methoxy signal enables one to calculate a factor that, when multiplied by the area of the main methoxy peak (21111 and 12111 sequences), will give the total area of the homopolymer methoxy signal; this factor was found to be 1.38 ± 0.06. For PMMA blends in which aromatic shielding is present, the determination of a factor that relates the total area of the homopolymer methoxy signal to that of the main peak located at approximately 3.57 ppm will become essential.

2.5. Line Shape of the PMMA–4VP Methoxy Groups in the Blend. For a blend of PMMA with another polymer containing aromatic groups, the line shape for the methoxy group indicates that it is composed of two superimposed signals, i.e., the unshielded methoxy signal (≅3.57 ppm) and the shielded methoxy signal (≅3.52 ppm). This is illustrated in Figure 2 for an equimolar blend of PS–SSA (10 mol %) of MW ≅ 10^4 with PMMA–4VP in DMSO-d_6 at 85 °C (contact time = 30 min). It should be pointed out that a shoulder is also present for the signal arising from the shielded methoxy groups. Furthermore, a comparison of the methoxy signal in the homopolymer at 85 °C (Figure 1) with that obtained for the blend at the same temperature (Figure 2) clearly indicates that the shoulder in the homopolymer methoxy signal, located at approximately 3.52 ppm, lies at approximately the same position as that of the shielded methoxy signal, and since the latter is quite large, the shoulder can appear buried.

This presents us with a major complication for the quantitative analysis of the areas due to the unshielded and shielded methoxy groups. A simple deconvolution into two Gaussians or two Lorentzians would not be correct in this particular case, since we know that the unshielded peak is composed of the peak and the shoulder; therefore, we cannot reconstruct the unshielded peak by itself. However, one does have information related to the relative areas of the shoulder and the unshielded peak.

For convenience, it was judged advantageous not to subtract the shoulder area from that of the shielded peak but instead to add it to that of the unshielded signal. Furthermore, from the relative area of the unshielded methoxy peak, one can obtain the concentration of the pure methoxy in solution at any given time. This concentration is, in fact, the only parameter required to establish the time–concentration curves.

The procedure that was adopted for the mixture of the two copolymers consists of the following steps: The two peaks for the spectrum were deconvoluted into two Lorentzian bands, and then the relative percent area of the unshielded methoxy group signal to the total area of the methoxy signal was calculated. Multiplication of the percent area of the unshielded methoxy peak by the factor determined in the previous section (1.38 ± 0.06) gives one the total percent area of the unshielded methoxy signal.

Recently, the validity of that procedure, for the blends, was ascertained by deconvoluting several methoxy line shapes using four Lorentzian bands, i.e., two for the unshielded and the shielded main peaks and two for their respective shoulders. The Jandel Scientific PeakFit program (version 3.1) was used for that purpose (see Figure 2). The relative areas of the unshielded methoxy line shape (main peak + shoulder) to the one for the shielded methoxy line shape were found to be within ±2% of those obtained with the earlier described procedure.

2.6. Application of the Deconvolution to a Typical Line Shape for Shielding. In order to minimize the acquisition time, ^{1}H NMR spectra were monitored for the spectral range included between 3.9 and 2.9 ppm. The line shape of the acquired spectrum is always composed of three major signals, i.e., the unshielded (≅3.57 ppm) and the shielded (≅3.52 ppm) methoxy group signal and the signal due to traces of water (≅3.15 ppm). Using a parabolic base line, the two overlapping methoxy signals and the water peak were deconvoluted as three Lorentzian bands. In all cases, a correlation equal to or greater than 0.995 was achieved.

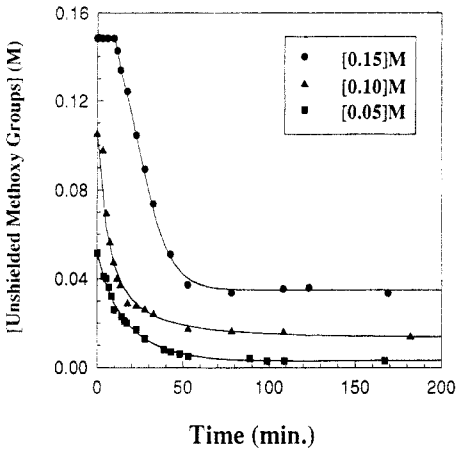

Figure 3. Time–concentration curves for various equimolar starting concentrations of PMMA–4VP with PS–SSA (10 mol %) of MW = 10^5, at 85 °C. The concentrations refer to the unshielded methoxy groups.

Thus, it can be concluded that there is no significant difference between the experimental and the deconvoluted line shape. Furthermore, the end value of the χ^2 obtained by the deconvolution process qualitatively indicates that the maximum error in the area of individual bands is on the order of ±2.5% (confidence level of 95%).

From these individual areas, the unshielded methoxy group concentration was calculated as described in the previous section and the time–concentration curves were obtained. The experimental parameters having an influence on the kinetic process were investigated for two PS–SSA samples of molecular weights of 10^5 and 10^4, i.e., for materials which yielded a resolvable ^{1}H NMR shielded methoxy signal in the blend.[14] A typical set of time–concentration curves, for various equimolar starting concentrations (a_0) of PS–SSA (MW = 10^5) at 85 °C, can be seen in Figure 3. Two things are worth noting about these curves. First, an induction period exists for most of the time–concentration curves, i.e., before the shielding process starts. This period varies between 1 and 10 min, and generally increases with increasing total concentration and MW, while it decreases with increasing SSA content and temperature. This induction period generally indicates that the reaction is composed of a series of reactions and that a rate-determining step is present.[27,28] Second, the shielding process does not go to completion within the experimental time frame. The concentration of the shielded methoxy groups at which the reaction reaches the equilibrium state (X_e) varies as a function of the studied parameters. However, the ratio of the X_e value to a_0 (multiplied by 100) is a qualitative criterion that indicates the extent of the overlap between the two dissimilar coils. For the concentration curves reported in Figure 3, the ratio of the a_0 values (0.05, 0.10, and 0.15 M) to their respective X_e values (0.047, 0.092, and 0.11 M) is equal to 94, 84, and 73%. This ratio indicates that, for this particular system, the extent of shielding decreases with increasing initial PS–SSA concentration (a_0). This behavior will be discussed in greater detail in the section dealing with quantitative kinetics.

3. Kinetic Data Treatment

There are many methods which can be used to determine the order of a reaction.[27,28] Since the coil overlap process is composed of more than one simple reaction, the differential method is the most suitable for the analysis of the time–concentration curves.[28,29] However, it should be stressed that there are a number of others.[30]

3.1. Differential Method. In the differential method, which was originally suggested by van't Hoff,[31] the actual reaction rates can be determined by measuring the slope of the concentration–time curves. The rate may be related to the concentration of a reactant by eq 1.

$$v = kc^n \tag{1}$$

where v is the velocity (dc/dt), k is the rate constant, c the concentration, and n the order of the reaction. Taking the natural logarithms yields

$$\ln v = \ln k + n \ln c \tag{2}$$

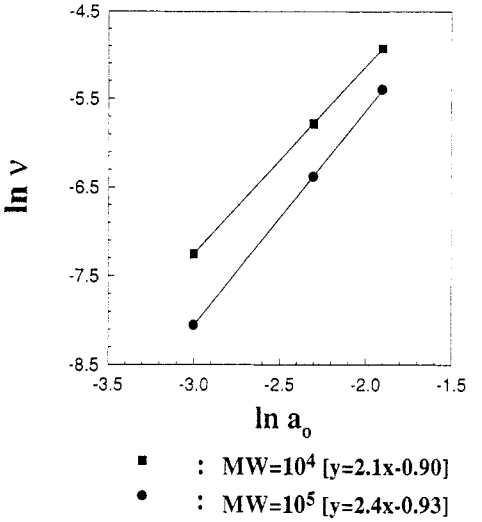

Figure 4. Determination of the true order (n_c) for equimolar blends of PMMA–4VP with PS–SSA (10 mol %) (MW = 10^4 and MW = 10^5) at 85 °C.

If the velocity is measured at various initial concentrations (a_0) and a log–log plot of the initial rate of reaction against the initial concentration is prepared, one should have a straight line with a slope equal to the order of the reaction. This procedure of dealing with initial rates avoids possible complications due to interference by products and leads to an order which corresponds to the simplest type of situation. In view of this, Letort[32] has referred to the order determined in this way as the order with respect to concentration or the true order (n_c).

The second procedure involves considering a single run and measuring slopes at various times corresponding to different values of the reactant concentrations. For a double-logarithmic plot of the rate of reaction as a function of the corresponding reactant concentrations, the slope is equal to n_t, which can be referred as the order with respect to time, because the time is now allowed to vary.

Comparing these two orders (n_t and n_c) can help us to draw some conclusions about the mechanism. In n_c is equal to n_t, it is an indication that there is no complexity in the mechanism. If the order n_c is greater than n_t, the reaction is said to be autocatalytic or that the mechanism is complex and that it involves more than one simple reaction step. If the order n_t is greater than the true order n_c, it means that some intermediate in the reaction is acting as an inhibitor.[27]

3.2. Determination of the True Order (n_c). The true order was determined for two series of experiments utilizing equimolar blends (at individual polymer concentrations of 0.05, 0.10, and 0.15 M) containing respectively PS–SSA (10 mol %) of MW ≅ 10^4 or MW ≅ 10^5, to which the PMMA–4VP was added. Figure 4 is a plot of ln v vs ln a_0, as described in eq 2, for the two sets of experiments. From the slope of this linear equation, one can obtain the true order of the reaction (n_c). Thus, for runs utilizing equimolar mixtures of PS–SSA of MW = 10^4 and MW = 10^5, n_c is equal to 2.1 ± 0.1 and 2.4 ± 0.1, respectively.

3.3. Determination of the Order According to Time (n_t). The determination of n_t, described previously, involves the measurement of tangents from a concentration–time curve. These determinations are fraught with experimental uncertainties. As a result of this, the determination of n_t from independent kinetic runs usually

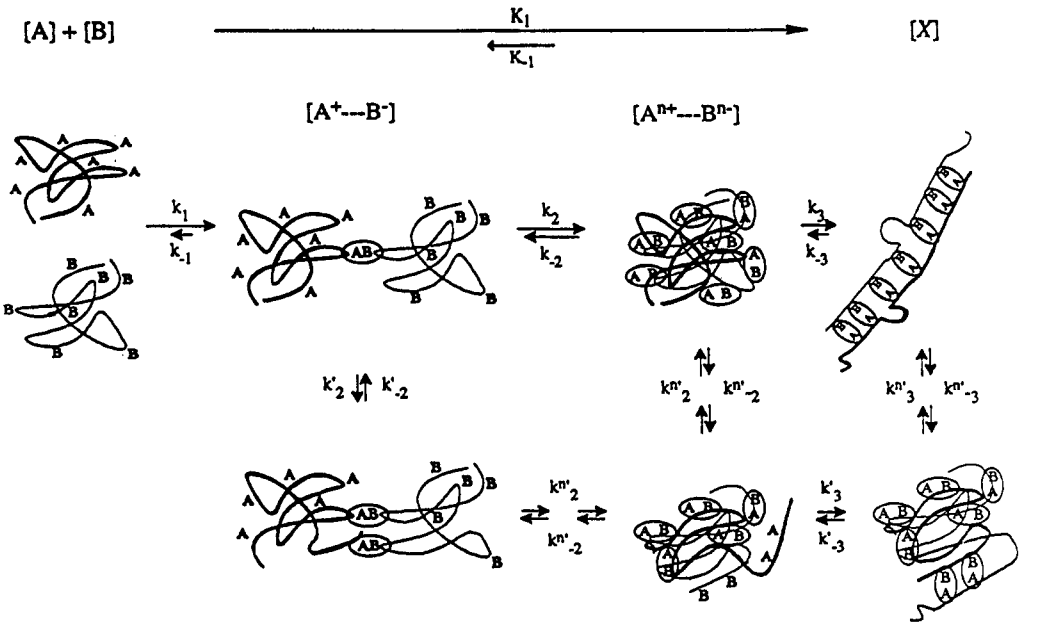

Figure 5. Diagram illustrating the proposed mechanism for the coil overlap process between two dissimilar chains of equivalent MW and ion content. Different line thicknesses represent the different copolymer chains (PMMA–4VP and PS–SSA), PMMA–4VP being the thicker of the two. The letters A (4VP) and B (SSA) denote the pendant ionic groups. The oval indicates that proton transfer has occurred and that the A and B groups are interacting. The length of the arrows roughly shows the rate of the reactions relative to one another.

leads to significant discrepancies between the various determinations. To avoid that pitfall, a standard procedure described in ref 23 was used. Briefly, it consists of systematically measuring the tangent on a fitted concentration–time curve at the same concentrations, i.e., 25%, 50%, and 75% of a_o.[27] Using this procedure, the mean values of n_t were obtained for the two series of equimolar blends described in the previous section. These values are equal to 1.2 ± 0.1 and 1.1 ± 0.1 for the blends containing PS–SSA (10 mol %) of MW $\cong 10^4$ and MW $\cong 10^5$, respectively. Thus, the order according to time obtained in both cases is lower than the true order. These values indicate that both reactions follow an apparent first-order scheme and, by extension, can be characterized by the same mechanism. This behavior is not unexpected, since the addition or the exchange reaction between polyelectrolytes usually follows a multistage process that can be characterized by an apparent first-order scheme.[18]

3.4. Comparison between n_t and n_c. The fact that the order with respect to time (n_t) is lower than that with respect to concentration (n_c) clearly shows that the mechanism is complex and that it involves more than one reaction. The facts that the coil overlap reaction proceeds through a multistage process[14,18] and that it involves two competing reactions[14] are the types of complications that lead to the observed discrepancy between n_c and n_t. Moreover, the determination n_t ($\cong 1$) shows that the global process must be characterized by a first-order reaction, even though n_c ($\cong 2$) indicates that the early stages of the coil overlap process proceed through a second-order scheme. These findings are important, since they will be used in the formulation of the global mechanism for the coil overlap process.

3.5. Mechanism for the Coil Overlap Process. Before suggesting a mechanism, however, it is important to review all the experimental observations that can be used to justify the mechanism. It is well-known that most proton-transfer reactions can be characterized as very rapid processes in which equilibrium is established essentially instantaneously.[18,33] From other studies, on model compounds in DMSO, it is known that the proton transfer from relatively weak acids (carboxylic or sulfonic) to the nitrogen atom of a substituted pyridine ring is fast ($<10^{-7}$ s)[33,34] and that it occurs when the two species are at distance on the order of 10–100 Å.[33] Thus, one can expect, for the present system, an analogous behavior for proton transfer from the SSA to the 4VP.

From the present experimental results, it can be suggested that each step of the complete coil overlap process is fully reversible and that therefore all the forward reactions contained in the mechanism must have their opposed backward reactions. Generally, the solutions are dilute. This implies that, at $t = 0$, the coils must be separated by a relatively large distance. A crude estimate of these distances can be obtained. For a total concentration of 0.05 M, they are on the order of 200 and 100 Å for mixtures containing PS–SSA samples of molecular weights of 10^5 and 10^4, respectively. The steps outlined in the discussion below are summarized in Figure 5. The reader may wish to consult this figure while reading the subsequent section.

Since the solutions are quite dilute, when two dissimilar chains collide, or segments are at a distance of less than 10 Å, proton transfer from a sulfonic acid group of the PS–SSA (B) chain to a vinylpyridine group of the PMMA–4VP (A) chain can occur. As soon as even one such event has taken place, one can assume that the two dissimilar chains form a complex and that the shielding process can now proceed between the two dissimilar chains within that complex. This is valid for two dissimilar chains of equivalent molecular weights. The formation of that initial complex [A$^+$—B$^-$] is the first step (initiation) of the proposed mechanism (having a rate constant k_1).

As soon as this initial complex is formed, a cascade reaction will be initiated, and most of the remaining protons of the SSA groups from the PS–SSA chain will be transferred more or less randomly to the nearest VP units in the complex. This random ion-pairing reaction between the two dissimilar chains involved in the initial complex constitutes the second step of the mechanism (characterized by rate constant k_2). In the previous study, Natansohn and Eisenberg[12] concluded that the vast majority of the protons from the SSA were interacting with the pyridine rings of the PMMA–4VP chains, even in the early stages of the mixing process. Thus, the formation of this complex ([A^{n+}—B^{n-}]) is rapid and is mostly complete by the time

the first ^{1}H NMR spectrum is acquired (<2 min). There is a strong electrostatic interaction between the chains. However, it must be stressed that the vast majority of the methoxy groups are not yet shielded at that point.

The third step of the mechanism can be attributed to the spatial reorganization of the two dissimilar chains involved in the $[A^{n+}—B^{n-}]$ complex (with a rate constant k_3). This reorganization of the complex is a slow process dictated, in part, by the segmental motions of the chains in solution. Some of the ion pairs in the $[A^{n+}—B^{n-}]$ complex will come apart and reform in such a way as to form a "ladder"-like complex (X). Thus, the presence of the shielded methoxy signal, observed in ^{1}H NMR, can be interpreted as the appearance of a certain quantity of the ladder complex in the solution. These three steps can be represented by the following equations

(1) initiation

$$A + B \underset{k_{-1}}{\overset{k_1}{\rightleftarrows}} [A^+—B^-]$$

(2) cascade reaction

$$[A^+—B^-] \underset{k_{-2}}{\overset{k_2}{\rightleftarrows}} [A^{n+}—B^{n-}] \quad (3)$$

(3) spatial reorganization

$$[A^{n+}—B^{n-}] \underset{k_{-3}}{\overset{k_3}{\rightleftarrows}} X$$

The overall reaction is obtained by adding the three equations of set (3)

$$A + B \underset{K_{-1}}{\overset{K_1}{\rightleftarrows}} X \quad (4)$$

where K_1 and K_{-1} are the rate constants for the global forward and backward reactions, respectively.

Using the steady-state method and after some rearrangement, one can obtain the equation for the net rate of production of X.[23]

$$\frac{dX}{dt} = \frac{k_2k_3}{k_{-2}+k_3}(a_o - X_e) - k_{-3}\left(1 - \frac{1}{k_2+k_3}\right)X_e \quad (5)$$

where a_o is the initial concentration of PMMA–4VP, and X_e is the equilibrium concentration of X. From the previous discussion (also see Figure 5), an additional set of equalities can be obtained

$$k_2 \gg k_{-1}$$
$$k_{-2} \gg k_3 \quad (6)$$
$$k_2 \gg k_3 > k_{-3}$$

Using the three equations of set (6), eq 5 becomes

$$\frac{dX}{dt} = \frac{k_2k_3}{k_{-2}}(a_o - X_e) - k_{-3}X_e \quad (7)$$

Substitution of k_2k_3/k_{-2} ($\cong K_1$) and k_{-3} ($\cong K_{-1}$) with the symbols of eq 4 yields an equation which is identical to the one derived from a mechanism in which two first-order reactions are opposing each other.

$$\frac{dX}{dt} = K_1(a_o - X_e) - K_{-1}X_e \quad (8)$$

The integration of eq 8 is well-known. The expressions for the rate constant of the forward reaction (K_1) and for the overall reaction ($K_1 + K_{-1}$) as a function of the equilibrium concentration of X ($=X_e$) are respectively

$$K_1 = \frac{1}{t}\frac{X_e}{a_o}\ln\left(\frac{X_e}{X_e - x}\right) \quad (9)$$

$$K_1 + K_{-1} = \frac{1}{t}\ln\left(\frac{X_e}{X_e - x}\right) \quad (10)$$

By expressing the data from the time–concentration curves as suggested by eq 9, i.e., by plotting the right-hand side of eq 9 as a function of time, one can obtain the rate constant K_1 from the slope. Using the same procedure, one can obtain the rate constant K_T ($=K_1 + K_{-1}$) from eq 10. The rate constant K_{-1} can then be calculated by subtracting K_1 from K_T.

From eq 7, it is clear that only the rate constants k_2 and k_{-2} (random occurrence of proton transfers) and k_3 (spatial reorganization) will have a major influence on the apparent rate constant (K_1) characterizing the forward reaction. For the backward reaction, only k_{-3} will have a major effect on the observed apparent constant K_{-1}.

Application of eq 9 enables one to obtain the rate constants for the mixing process. However, these are only apparent rate constants, since they contain all the individual rate constants included in the overall process. Thus, the application of eq 9 can be envisaged as a mathematical scheme and enables one to obtain quantitative information on the system without having to characterize all the individual rate constants of the process.

3.6. Application of the First-Order Scheme to the Time–Concentration Curves. The time–concentration curves for the blends were graphically analyzed using eqs 9 and 10. Typical plots that were used to determine the first-order rate constants can be found in Figure 6. These plots were obtained for equimolar mixtures (0.05 M) containing PMMA–4VP with PS–SSA (10 mol %) of MW = 10^5. The equilibrium concentration of the shielded methoxy groups (X_e) for that particular blend is equal to 0.047 M and is attained after ≅75 min, i.e., when the variation in concentrations is less than 5% of the equilibrium concentration. The correlation coefficient obtained from the determination of K_1 for this mixture is equal to 0.996. For all the studied mixtures, the mean correlation coefficients are equal to 0.988. This value confirms that a mechanism containing two first-order opposing reactions is suitable to describe the global process. It is important to note that the induction periods that are observed in the time–concentration curves were not included in the linear regression, since during this time period the concentration of the product either remained below the experiment limit of detection or was simply not produced at all.[27-29]

4. Quantitative Kinetics. Results and Discussion

4.1. Introduction. This section will examine the kinetic results obtained in the studies of the effects of various experimental parameters on the shielding and deshielding processes for mixtures of the two copolymers. As previously mentioned, the data gathered so far on the coil overlap process of the copolymer mixtures lead to the conclusion that the mechanism is analogous to an overall reaction containing two first-order reactions that are opposing one another. Using the procedure described in the previous section, one can obtain the rate constants for

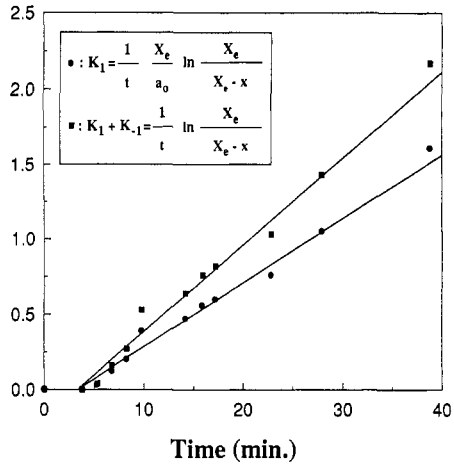

Figure 6. Plots of eqs 7 and 8 for an equimolar mixture of PMMA–4VP with PS–SSA (10 mol %) of MW = 10^4, at 85 °C. The DMSO-d_6 solution contains 2.5 mg of each copolymer per 0.5 mL (0.05 M).

each process. A comparison of these calculated rate constants will enable one to quantify the influence of each experimental parameter on the overall process. For each blend, the apparent rate constants for the processes were determined, i.e., shielding (K_1), deshielding (K_{-1}), and the total process (K_T). The ratio of K_1 to K_{-1} (k_{eq}) was calculated. This ratio should be considered as an indication of how much material has gone through spatial reorganization and should not be confused with the "true" equilibrium constant, since K_1 and K_{-1} are apparent rate constants. It is important to recall that, for all these mixtures, the PMMA–4VP copolymer is identical; i.e., the 4VP content is equal to 11 mol %, and the MW is 10^5.

4.2. Parameters Affecting the Shielding Process for Blends Containing PS–SSA of MW = 10^5. In this section, three experimental parameters influencing the coil overlap process will be discussed. For these blends, the MW of the second copolymer involved in the mixing process (PS–SSA) remains constant (10^5), while the other experimental parameters are varied one at a time. In sections 4.2.1 to 4.2.3, the influence of the temperature, the SSA content, and the total polymer concentration will be discussed. It is important to note that, in order to form the [A^{n+}—B^{n-}] complex, only one PS–SSA chain per PMMA–4VP chain is required, since both chains have a similar molecule weight. This implies that the ladder-like complex (X) will probably contain only two dissimilar chains that have gone through spatial reorganization.

4.2.1. Temperature. It was previously shown that temperature has two opposing effects which are competing during the coil overlap process.[14] On the one hand, an increase in temperature favors molecular motions and therefore increases the rate at which the two dissimilar chains find one another in solution. It may also favor, to a certain extent, the spatial reorganization of the ladder complex. However, an increase in temperature will effectively decrease the relative importance of the Coulombic interactions between the ions, and therewith the driving force for the mixing process.

Therefore, on the basis of the proposed mechanism, two possible cases can be envisaged in terms of their effect on the apparent rate constant of the shielding process, i.e., K_1 ($\cong(k_2\ k_3)/k_{-2}$). First, if the disruptive effects of the molecular motions of the two dissimilar chains involved in the [A^{n+}—B^{n-}] complex are not dominant, it is expected that the value of K_1 will increase as the temperature increases. However, if the disruptive effects are dominant, the value of the apparent rate constant for the shielding process will decrease, since it is a product of two rate constants (k_2 and k_3) for two processes that will be inhibited by an increase in temperature. The deshielding rate constant K_{-1} ($\cong k_{-3}$) should have approximately the same value, since the temperature is not high enough to cause a major disruption of the Coulombic interactions.[14] Consequently, for a certain temperature range, the value of the rate constant for the total coil overlap process (K_T) will show the same trend as K_1, since it is a sum of one quantity that is variable (K_1) and another which is constant (K_{-1}).

Table 2. Effect of Temperature: Rate Constants for Equimolar Blends (0.10 M) of PMMA–4VP with PS–SSA of 10 mol % (MW = 10^5)

temp (°C)	rate constant (min^{-1}) total (K_T)	shielding (K_1)	deshielding (K_{-1})	K_1/K_{-1} (k_{eq})
70	0.020	0.011	0.009	1.2
75	0.028	0.014	0.014	1.0
80	0.065	0.055	0.010	5.5
85	0.102	0.089	0.013	6.8
95	0.139	0.118	0.021	5.6

Equimolar mixtures (0.10 M in repeat units of each copolymer) of PMMA–4VP with PS–SSA of 10 mol % were used to perform this study at five temperatures. The values of the relevant rate constants are reported in Table 2.

From these results, one can see that, as the temperature increases, the values for the shielding and the total rate constants increase monotonously. On the other hand, the value of the rate constant for the deshielding process remains almost constant within experimental error up to 95 °C. The values obtained for k_{eq} show a significant increase at 80 °C; then this value levels off when the temperature increases further.

These results show that, in this system, an increase in the temperature favors the shielding process. At 95 °C, the disruptive effects of the segmental motions of the chains become strong enough to perturb the Coulombic interactions between the ion pairs, leading to a decrease in the quantity of ladder-like complex formed when steady state is achieved, but not strong enough to inhibit the shielding process.

4.2.2. SSA Content. Since the Coulombic interactions between the ions are the driving force for the mixing process, it is expected that the value of the apparent shielding rate constant should increase with increasing SSA content. This increase is obviously due to the presence of a greater number of reactive sites on the PS–SSA chain. It should be recalled that the apparent rate constants in eq 9 are related to the concentration of polymer chains, not of the functional groups. Clearly, the probability of the occurrence of proton transfer increases with increasing SSA content, which implies that rate constant k_2 will increase. One can also anticipate that the value of k_{-2} will decrease, while the value of k_3 should remain almost unchanged with increasing SSA contents, since k_3 is mostly a function of the segmental motions of the chains; adding more ions on a PS chain should not have a major effect on the rate constant k_3. Furthermore, from section 4.2.1, it is known that at 85 °C no significant disruptions occur to the ion–ion interactions. Thus, two kinds of behavior can be envisaged for K_{-1}. In the case of major disruptions, values of K_{-1} will remain constant or increase with increasing SSA contents. On the other hand, if the disruptive effects are minor, it is expected that the values of K_{-1} will decrease. Thus, all the rate constants which contribute to K_1 behave so as to lead to an increase of the value of the rate constant as the SSA ion content increases.

Table 3. Effect of the SSA Content: Rate Constants for Equimolar Blends of PMMA-4VP with PS-SSA (MW = 10^5) at 85 °C

SSA content (mol %)	ratio (% 4VP/ % SSA)	rate constant (min^{-1}) total (K_T)	shielding (K_1)	deshielding (K_{-1})	K_1/K_{-1} (k_{eq})
7.7	1.4	0.084	0.054	0.030	1.8
10.0	1.1	0.102	0.089	0.013	6.8
14.7	0.8	0.166	0.163	0.003	55

Table 4. Effect of the Total Polymer Concentration: Rate Constants for the Total Polymer Concentration Range, for Equimolar Blends of PMMA-4VP with PS-SSA (10 mol %) (MW = 10^5) at 85 °C

total polym concn (M)	rate constant (min^{-1}) total (K_T)	shielding (K_1)	deshielding (K_{-1})	K_1/K_{-1} (k_{eq})
0.10	0.084	0.042	0.015	2.8
0.20	0.102	0.089	0.013	6.8
0.30[a]	0.044	0.034	0.010	3.4

[a] Indicates precipitation occurs during the experiment.

Three equimolar blends (0.10 M) of PMMA-4VP with PS-SSA of various SSA contents at 85 °C were used to perform this study. The values of the rate constants were determined. These values are summarized in Table 3. From these results, one can see that, as the ion content of the PS-SSA chains increases, the shielding and the total rate constants are increasing. On the other hand, the values of the constants for the deshielding process decrease drastically with SSA content. From the k_{eq}, one is able to observe that its value increases with increasing SSA contents, and a plot (not shown) suggests that the increase is exponential with an exponent of 5.3 and a correlation coefficient of 0.9996.

These results show that, in this system, an increase in the SSA content will favor the shielding process, accompanied by a decrease in the apparent deshielding rate constants. This trend for the apparent deshielding rate constants also suggests that, at 85 °C, the disruptive effects of the temperature are minor.

4.2.3. Total Polymer Concentration. It was shown in the previous paper that, after the induction period, the rate of the coil overlap process increased as the polymer concentration increased. It was concluded that the coil overlap process, during this stage, was governed by the spatial reorganization of the two dissimilar chains. Thus, it is expected that the values of the apparent shielding (K_1) and deshielding rate constant (K_{-1}), should increase with an increase in the total polymer concentration. This increase is obviously due to the presence of a greater number of chains in solution. Furthermore, for these high molecular weight polymers, it is conceivable that occasional "castastrophic" pairing of the dissimilar chains will occur at high concentration, leading to the formation of microgels (pseudonetwork). This behavior has been observed for systems in which interpolymer complexes are formed.[35] Due to this phenomenon, a fraction of the chains becomes insoluble. This leads to the reduction of the expected equilibrium concentration of X and, by extension, to the reduction of K_1.

Three equimolar blends (0.05, 0.10, and 0.15 M) of PMMA-4VP with PS-SSA of 10 mol % at 85 °C were used to perform this study. For these three blends, values of the rate constants are reported in Table 4. One can see from these results that, as the total concentration of the two copolymers chains increases up to 0.20 M, the shielding and the total rate constants are increasing. On the other hand, the rate constant of the deshielding process remains approximately constant. This is illustrated by the trend of the calculated values of k_{eq}, which are increasing as the concentration is increased. For mixtures containing a total polymer concentration of 0.30 M, precipitation occurs, which makes a kinetic interpretation of the data meaningless.

These results show that, in this system, an increase in concentration will accelerate the shielding process. On the other hand, the deshielding process is not affected by an increase in concentration. Moreover, since precipitation occurs for total concentrations of 0.30 M, it seems that, for this PS-SSA of a MW of 10^5, the ladder-like complex will be formed only at relatively low concentrations, which avoids the formation of a pseudonetwork.

4.3. Parameters Affecting the Shielding Process for Blends Containing PS-SSA of MW = 10^4. As in the previous section the parameters of the PMMA-4VP chains and the molecular weight of the PS-SSA (10^4) will be kept constant, while the other experimental parameters, i.e., the temperature, the SSA content, and the total polymer concentration, will be varied. The results will be discussed in sections 4.3.1 to 4.3.3.

It is important to note that, in this case, in order to form the $[A^{n+}—B^{n-}]$ complex, more than one PS-SSA (chain ($\cong$10) per PMMA-4VP will be required for neutralization. This implies that the ladder-like complex (X) will probably contain several independent sections that have gone through spatial reorganization, which was not the case when the two dissimilar chains had a similar molecular weight. Thus, compared to a mixture containing a relatively high molecular weight PS-SSA, one can expect that a shorter period of time will be needed in order to reach the equilibrium shielded methoxy group concentration (X_e); i.e., higher values of K_1 will be encountered.

Obviously, for these low PS-SSA MW blends, a faster formation of the ladder-like complex does not imply that the shielding is as effective as in the case of the high MW blends. Here, most probably the $[A^{n+}—B^{n-}]$ complex will be formed without a perfect match in contour lengths between the dissimilar chains. The ladder-like complex is expected to contain more defects, since during its formation, it is very unlikely that all the strongly interacting groups of two (or more) PS-SSA chains will break at the same time and realign in order to form a quasi perfect ladder. Thus, for the blends containing PS-SSA chains of low MW, the experimental X_e values are expected to be lower than those observed in the previous section, and, by extension, higher K_{-1} values can be anticipated.

4.3.1. Temperature. As mentioned earlier, for blends involving relatively low molecular weight PS-SSA copolymers, it is reasonable that an increase in temperature should increase the value of the apparent shielding constant, K_1, since the chains will be able to go through spatial reorganization more rapidly as blends formed by two dissimilar chains of equivalent MWs. However, the disruptive effects of the temperature may be strong enough to break more of the specific ion-ion interactions than in the case of a high molecular weight PS-SSA. Thus, the spatial reorganization will be hampered due to the lack of cooperative motions between the chains yielding smaller K_1 values.

Using the same conditions as described in section 4.2.1, values of the relevant rate constants were determined and are reported in Table 5. From these results, one can see that, as the temperature increases, the values for the shielding and the total rate constants are increasing up to 80 °C. On the other hand, the value of the rate constant for the deshielding process remains almost constant within experimental error. Consequently, values obtained for the equilibrium constants (k_{eq}) show the same trend as

Table 5. Effect of Temperature: Rate Constants for Equimolar Blends (0.10 M) of PMMA-4VP with PS-SSA (10 mol %) (MW = 10^4)

temp (°C)	rate constant (min^{-1}) total (K_T)	shielding (K_1)	deshielding (K_{-1})	K_1/K_{-1} (k_{eq})
70	0.060	0.040	0.020	2.0
75	0.089	0.066	0.023	2.9
80	0.100	0.078	0.022	3.5
85	0.080	0.058	0.022	2.6
95	0.060	0.034	0.026	1.3

Table 6. Effect of the SSA Content: Rate Constants for Equimolar Blends (0.10 M) of PMMA-4VP with PS-SSA (MW = 10^4) at 85 °C

SSA content (mol %)	ratio (% 4VP/ % SSA)	rate constant (min^{-1}) total (K_T)	shielding (K_1)	deshielding (K_{-1})	K_1/K_{-1} (k_{eq})
5.3	2.1	0.027	0.010	0.017	0.6
8.3	1.3	0.025	0.013	0.012	1.1
9.2	1.2	0.060	0.036	0.017	2.1
10.5	1.1	0.079	0.057	0.022	2.6
13.8	0.8	0.170	0.120	0.050	2.4

K_1, i.e., increasing up to 80 °C and then decreasing as the temperature increases further.

These results show that, in this system, an increase in temperature will favor the shielding process up to 80 °C. However, for higher temperatures, the disruptive effects of the segmental motions of the chains become dominant over the Coulombic interactions between the ion pairs. The decrease in the apparent shielding rate constant for temperature higher than 80 °C can be attributed mostly to that effect.

A comparison of the rate constants discussed above with those of section 4.2.1 enables one to elucidate some of the MW effects on the coil overlap process. The specific effects of the temperature can be obtained from a comparison of the values of the apparent rate constants K_1 and K_{-1} reported in Tables 2 and 5. For the high molecular weight mixtures (Table 2), one can see that the values of K_1 increase monotonously with temperature. By contrast, for the low molecular weight mixtures (Table 5) these values increase up to 80 °C and then decrease for higher temperatures. This implies that the disruptive effects induced by temperature in this range will not inhibit the shielding process for blends containing PS-SSA chains of high molecular weights. However, at much higher temperature the disruptive effect can be expected.[14] By contrast, for low molecular weight mixtures a relatively low threshold in temperature exists at which the shielding process will be hampered. From Tables 2 and 5, one can see that the temperature does not have a major effect on K_{-1}. However, it should be pointed out that the values of K_{-1} are always higher for the low MW mixtures. This indicates that the equilibrium concentration of shielded methoxy groups (ladder-like complex) is higher for the high MW mixtures.

For mixtures containing high molecular weight PS-SSA chains, it can be concluded that an increase in temperature will favor the global coil overlap process but not necessarily the formation of the ladder-like complex. For the low molecular weight mixtures it is clear that at high temperatures the global process is inhibited. Thus, to obtain the largest quantity of shielded methoxy groups for a given mixture, two conditions must be met. First, the molecular weight of the PS-SSA chain must be high enough to counteract the disruptive effects of the temperature. Second, the temperature must be high enough to favor the spatial reorganization of the two dissimilar chains without inhibiting the process, i.e., up to 85 °C.

4.3.2. SSA Content. The Coulombic interactions between the ions are the driving force for the mixing process. Thus, using the same arguments that were used in section 4.2.2., one can expect K_1 to increase with increasing SSA contents. Furthermore, from section 4.3.1, it is known that, at 85 °C and above, significant disruptions occur to the ion–ion interactions. Thus, two kinds of behavior can be envisaged for K_{-1}. In the case of major disruptions, values of K_{-1} will remain constant or increase with increasing SSA contents, since this apparent rate constant is, to a certain extent, a measure of the effectiveness of the shielding. On the other hand, if the disruptive effects are minor, it is expected that the value of K_{-1} will decrease.

Five equimolar blends (0.10 M) of PMMA–4VP with PS–SSA of various SSA contents at 85 °C were used to perform this study. For these five blends, the rate constants were determined and are reported in Table 6. One can see from the table that, as the ion content of the PS–SSA chains increases, the shielding, the deshielding, and the total rate constants increase. However, the rate constant of the shielding process increases slightly more rapidly than that of the deshielding process. From the value of k_{eq}, one can see that its value increases until the ion content of the two dissimilar chains is equal and then levels off.

These results show that, in this system, an increase in the SSA content will favor the shielding process up to the point where the ion contents of the dissimilar chains are equal. On the other hand, the SSA contents do not affect the apparent deshielding rate constant for symmetrical mixtures or those in which the 4VP/SSA mole percent ratio > 1. However, when there is an excess of SSA groups in the mixture, the rate constant K_{-1} increases drastically. This observation can be rationalized by recalling a previous comment on the nature of this rate constant. K_{-1} can be directly related to the effectiveness or the extent of the shielding (X_e/a_o ratio); at equilibrium, since a_o remains constant, this implies that the value of the apparent rate constant will increase if the X_e values are decreased. Clearly, this means that, for asymmetric mixtures of low 4VP/SSA values, a smaller quantity of the ladder-like complex is formed than for symmetric mixtures. This may be due to the fact that, in asymmetric systems, the ladder complex is formed too rapidly, and since it is formed with a certain number of PS–SSA (≅10) chains per PMMA–4VP chain, these strongly interacting chains will, to a certain extent, prefer to undergo a minimum of spatial reorganization.

Overall, the formation of the ladder-like complex is favored by an increase of the SSA content. However, for the nonsymmetric mixture in which an excess of SSA groups is present, K_{-1} increases and the formation of the ladder-like complex is slightly inhibited.

As in the previous section, the MW effects on this parameter can be obtained from the values of the apparent rate constants K_1 and K_{-1} reported in Tables 3 and 6. The values obtained for the apparent rate constants K_1 for mixtures containing low and high molecular weight PS–SSA chains show that in both systems an increase in the SSA content accelerates the shielding process. For an equivalent ratio (% 4VP/% SSA in these tables), the subtraction of the K_1 values of Table 3 from those of Table 6 gives a constant value (≅0.4). This implies that an increase in the SSA content will produce the same effect on K_1, independent of the molecular weight. However, for systems containing high MW PS–SSA chains, the shielding process will be favored compared to those containing low MW chains. By contrast, the behavior of

Table 7. Effect of the Total Polymer Concentration: Rate Constants for Equimolar Blends of PMMA-4VP with PS-SSA (10 mol %) (MW = 10^4) at 85 °C

total polym concn (M)	rate constant (min^{-1}) total (K_T)	shielding (K_1)	deshielding (K_{-1})	K_1/K_{-1} (k_{eq})
0.10	0.018	0.011	0.007	1.5
0.20	0.079	0.057	0.022	2.6
0.30	0.250	0.170	0.080	2.1

the rate constants K_{-1} differs drastically for the two systems. For the low molecular weight system, the values of K_1 increase with increasing SSA contents, while for the mixtures containing high MW chains, the K_{-1} values decrease.

Thus, it can be concluded that, by increasing the SSA content, one will always increase the rate of the global process. However, the optimal quantity of shielded methoxy groups will be produced for a system containing two dissimilar chains of comparable and high molecular weights. This molecular weight effect is probably due to the existence of a match between the contour lengths of the two high MW dissimilar chains. Moreover, these high MW chains must bear a relatively large (or equivalent) quantity of SSA and 4VP on their backbone (≅10 mol %) in order to produce the highest quantity of shielded methoxy groups. A low concentration of functional groups leads presumably to a greater mean distance between the two dissimilar chains, which implies that a lower quantity of shielded methoxy groups is achieved at steady state.

4.3.3. Total Polymer Concentration. From the arguments of section 4.2.3, it is expected that the values of the apparent shielding rate constants should increase with increasing polymer concentration. On the other hand, K_{-1} values should remain constant or increase if occasional catastrophic pairing of the dissimilar chains occurs at high concentration.

Three equimolar blends (0.05, 0.10, and 0.15 M) of PMMA-4VP with PS-SSA (10 mol %) at 85 °C were used for this study. For these three blends, the relevant rate constants were calculated. These rate constants are reported in Table 7. This table shows that, as the concentration of the two copolymers chains increases, the shielding, the deshielding, and the total rate constants increase. However, the rate of the deshielding process increases more rapidly than that of the shielding process. This is clearly illustrated by the trend of the calculated values of k_{eq}, which first increase and then decrease as the concentration is increased.

These results show that, in this system, an increase in the total polymer concentration will favor the rates of the shielding and the deshielding processes. However, the value of K_{-1} increases more rapidly than that for K_1. An estimate of the initial distances between two dissimilar coils in solution gives a better picture of what is happening when the concentration is increased. For the mixtures containing total concentrations of 0.10 and 0.20 M, the average distances between two dissimilar chains are greater than the sizes of the coils themselves. However, this is not the case for the mixture containing a total concentration of 0.30 M, for which it can be calculated that the distance is smaller than the size of the coil. Thus, one can conceive that there is a threshold concentration above which the rate of formation of the ladder-like complex will be reduced. At this point, more than one PS-SSA chain can interact with a given PMMA-4VP chain (and possibly vice versa). This will result in occasional catastrophic pairing of chains that will lead to the formation of a (soluble) microgel. This species will, however, be highly entangled, the entanglement being reinforced by the strongly interacting ion pairs. It is conceivable that portions of this complex will not be able to go through spatial reorganization.

One can conclude that an increase in concentrations leads to an increase in the value of the rate constants. However, it seems that the pure ladder-like complex will be produced only for dilute solutions.

A comparison of the values of K_1 from Tables 4 and 7 enables one to understand the effects of the total polymer concentration on the shielding process, while a comparison between the K_{-1} values from these tables enables one to explain the effects of the total concentration on the deshielding process. These two independent comparisons can then be related to the global process. This discussion will exclude the mixtures in which precipitation occurs, i.e., those for which the total polymer concentration is 0.30 M for the blend containing the high molecular weight PS-SSA (10^5). However, it is clear that if the total polymer concentration is too high, the interpenetration of coils will inhibit the formation of the ladder-like complex. Moreover, this will lead to diminution of the equilibrium concentration of shielded methoxy groups.

The K_1 values for both systems exhibit the same trend, i.e., increasing with increasing polymer concentrations. Subtraction of the K_1 values reported in Table 4 from those of Table 7 for the systems containing total polymer concentrations of 0.10 and 0.20 M gives 0.31 and 0.32, respectively. Since, the values from these subtractions are almost equal, one can say that an increase in concentration has the same effect on both systems. However, for equivalent concentrations, systems containing two dissimilar chains of MW = 10^5 show higher values for the apparent rate of shielding. Thus, if the molecular weight of the PS-SSA chain is increased, the rate of the shielding process will also increase, in parallel with the effect of increasing the SSA content.

By contrast, increasing the total polymer concentation will produce opposite effects on the apparent deshielding constants for the two systems. From Table 7 (low MW PS-SSA chains), one can see that the values for K_{-1} increase with increasing concentrations. This behavior was rationalized in section 4.2.3 by invoking the formation of microgels (pseudonetworks) due to the serious interpenetration occurring for the polymer coils with increasing polymer concentrations. On the other hand, for mixtures containing PS-SSA of MW = 10^5, an increase in the concentration will not produce a major effect on the K_{-1} values. This indicates that an increase in concentration will only have a major effect on the deshielding process for the mixtures containing low MW PS-SSA chains.

Thus, one can conclude that in both systems an increase in the total polymer concentration will lead to an increase in the rate of the global process. However, this increase does not imply that more shielded methoxy groups will be present at steady state. On the contrary, for systems containing PS-SSA chains of MW = 10^4, the equilibrium concentration of shielded methoxy groups decreases with increasing concentration, while for mixtures containing PS-SSA chains of MW = 10^5, an increase in concentration leads to the precipitation of the product. This indicates that, in order to obtain an optimal concentration of shielded methoxy groups, the solution must be in the semidilute regime, i.e., without coil interpenetration at $t = 0$. Moreover, if the mixture is in the semidilute region, optimal shielding will be achieved with high molecular weight PS-SSA chains.

5. Conclusions

In this paper, a detailed mechanism was suggested for the global coil overlap process. It was established that in

the early stages the process follows a second-order scheme ($n_c \cong 2$). However, the global process is best characterized by an apparent first-order scheme ($n_t \cong 1$). The reaction mechanism consists of three distinct reversible steps. First, a proton transfer occurs from the SSA group (B) to the 4VP moiety (A), with a rate constant k_1, producing the first ion pair between the two dissimilar chains. Second, the two chains being relatively close to one another, the vast majority of the remaining protons of B are transferred to A. This step, with a rate constant k_2, leads to the formation of an interpolymer complex, [A^{n+}—B^{n-}], in which the ions are randomly paired. Third, through a spatial reorganization, with a rate constant k_3, the [A^{n+}—B^{n-}] complex forms the final product (X), in which the dissimilar chains are relatively well aligned. From the NMR point of view, the formation of this ladder-like complex leads to the gradual diminution of the original methoxy protons signal and to the appearance of a new signal originating from the shielded methoxy protons.

The two first steps of the mechanism are very rapid compared to last one, i.e., the spatial reorganization. Consequently, the third step is the rate-determinating step for this reaction. On the basis of this mechanism, a kinetic expression was derived. This kinetic expression was found to be similar to one for a much simpler reaction, i.e., a mechanism containing two opposing first-order reactions. The apparent constants associated with this mechanism, K_1 ($\cong (k_2k_3)/k_{-2}$) and K_{-1} ($\cong k_{-3}$), were used to analyze the experimental data. Evidently, the evaluation of the two global rate constants (K_1 and K_{-1}) does not provide information about the absolute values of each individual rate constant contained in the mechanism (k_n and k_{-n}). However, since the determinations of the rate constants for the two first steps (k_1 and k_2) are very tedious and on the order of the dead time of the best technique available (stop-flow fluorescence),[18] this approach can be envisaged as a satisfactory mathematical scheme to get kinetic information on the process.

The effects of the individual parameters on the coil overlap process can be summaried as follows: First, the high molecular weight PS–SSA chains (MW $\cong 10^5$) give the highest rate for the shielding process and, by extension, also for the global process. High molecular weight chains also lead to optimal production of species in which the methoxy groups are shielded, which is presumably due to the fact that the contour lengths of the two dissimilar chains are similar. However, this statement is only valid for the dilute or semidilute regimes, since it was observed that gelation was occurring for more concentrated solutions. Second, an increase in the temperature, in the SSA content, or in the total polymer concentration always increases the rate of the global process. Third, at high temperatures ($\cong$ 85 °C), the disruptive effects of temperature inhibit, to a certain extent, the formation of shielded methoxy groups. The extent of this disruption is molecular weight dependent; i.e., it causes a major disruption only in the case of low molecular weight PS–SSA chains. Finally, an increase in the SSA content or in the total polymer concentration produces a maximum concentration of shielded methoxy groups (X_e) only for blends containing high MW PS–SSA chains. By comparison to low MW blends, this behavior was rationalized by invoking a better match in total lengths that exists when the two dissimilar chains are of similar MW.

References and Notes

(1) Sultzberg, T.; Colter, R. J. *J. Polym. Sci., Polym. Chem. Ed.* **1970**, *8*, 2747.

(2) Krause, S. *J. Macromol. Sci., Rev.* **1972**, *C7*, 251.

(3) Klempner, D.; Frisch, K. C. *Polymer Alloys: Blends, Blocks, Grafts and Interpenetrating Networks*; Polymer Science and Technology; Plenum Press: New York, 1977; p 10.

(4) Paul, D. R.; Newman, S. *Polymer Blends*; Academic Press: New York, 1978; Vols. 1 and 2.

(5) Olabisi, O.; Robenson, L. M.; Shaw, M. T. *Polymer–Polymer Miscibility*; Academic Press: New York, 1970.

(6) Higgins, J. S.; Walsh, D. J. *Polym. Eng. Sci.* **1984**, *24* (8), 555.

(7) Schroeder, J. A.; Karasz, F. E.; MacKnight, W. J. *Polymer* **1985**, *26* (12), 1795.

(8) Smith, P.; Hara, M.; Eisenberg, A. *Current Topics in Polymer Science*; Hanser: New York, Vol. 1. Gao, Z.; Molnár, A.; Eisenberg, A. *Ionomers: Synthesis, Structure, Properties and Applications*; Van Nostrand-Reinhold: 1994, to be published.

(9) Zhao, Y.; Prud'homme, R. E.; Bazuin, C. G. *Macromolecules* **1991**, *24* (6), 1261. Zhao, Y.; Bazuin, C. G.; Prud'shomme, R. E. *Macromolecules* **1989**, *22* (9), 3788. Mattera, V. D., Jr.; Risen, W. M., Jr. *J. Polym. Sci., Polym. Phys. Ed.* **1984**, *22* (1), 67. Earnest, T. R.; MacKnight, W. J. *Macromolecules* **1980**, *13*, 844.

(10) Djordjevic, M. B.; Porter, R. S. *Polym. Eng. Sci.* **1983**, *23*, 650. Douglass, D. C.; McBrierty, V. J. *Polym. Eng. Sci.* **1979**, *19*, 1054.

(11) Chen, C. T.; Morawetz, H. *Macromolecules* **1989**, *22* (1), 159. Jachowicz, J.; Morawetz, H. *Macromolecules* **1983**, *15* (3), 828. Egan, L. S.; Winnik, M. A.; Croucher, M. D. *Polym. Eng. Sci.* **1986**, *26* (1), 15. Winnik, M. A.; Pekcan, O.; Chen, L.; Croucher, M. D. *Macromolecules* **1988**, *21* (1), 55. Peterson, K. A.; Zimmt, M. B.; Fayer, M. D.; Jeng, Y. H.; Frank, C. W. *Macromolecules* **1989**, *22* (2), 874. Thomas, J. W., Jr.; Frank, C. W.; Holden, D. A.; Guillet, J. E. *J. Polym. Sci., Polym. Phys. Ed.* **1982**, *20* (9), 1749. Frank, C. W.; Gashgari, M. A. *Ann. N.Y. Acad. Sci.* **1981**, 366 (*Lumin. Biol. Synth. Macromol.*), 387. Izumrudov, V. A.; Savitskii, A. P.; Bakeev, K. N.; Zezin, A. B.; Kabanov, V. A. *Makromol. Chem., Rapid Commun.* **1984**, *5*, 709.

(12) Natansohn, A.; Eisenberg, A. *Macromolecules* **1987**, *20* (2), 323.

(13) Sanders, J. K. M.; Mersh, J. D. *Progr. NMR Spectrosc.* **1982**, *15*, 353.

(14) Bossé, F.; Eisenberg, A., submitted for publication to *Macromolecules*.

(15) Stuckey, M.; Wyn-Jones, E.; Akasheh, T. *J. Chem. Soc., Faraday Trans. 1* **1987**, *83* (8), 2525. Lankhorst, D.; Leyte, J. C. *Macromolecules* **1984**, *17* (1), 93. Weiss, S.; Diebler, H.; Michaelli, I. *J. Phys. Chem.* **1971**, *75* (2), 267.

(16) Kabanov, V. A.; Zezin, A. B.; Izumrudov, V. A.; Bronich, T. K. *Makromol. Chem. Suppl.* **1985**, *13*, 137.

(17) Chen, H. L.; Morawetz, H. *Macromolecules* **1982**, *15*, 1445. Chen, H. L.; Morawetz, H. *Eur. Polym. J.* **1983**, *19*, 923.

(18) Bakeev, K. N.; Izumrudov, V. A.; Kuchanov, S. I.; Zezin, A. B.; Kabanov, V. A. *Macromolecules* **1992**, *25*, 4249.

(19) Duchesne, D. Ph.D. Thesis, McGill University, 1985.

(20) Burleigh, J. E.; McKinney, O. F.; Barker, M. G. *Anal. Chem.* **1959**, *31* (10), 1684.

(21) Makowski, H. S.; Lundberg, R. D.; Singhal, G. H. U.S. Patent 3,870,841, 1975.

(22) Erdi, N. Z.; Morawetz, H. *J. Colloid Sci.* **1964**, *19*, 708.

(23) Bossé, F. M. Sc. Thesis, McGill University, 1991.

(24) Marquardt, D. W. *Chem. Eng. Prog.* **1959**, *55*, 65.

(25) Marquardt, D. W. *J. Soc. Ind. Appl. Math.* **1963**, *11* (2), 431.

(26) Natansohn, A.; Maxim, S.; Feldman, D. *Eur. Polym. J.* **1978**, *14*, 283.

(27) Laider, K. J. *Chemical Kinetics*, 3rd ed.; Harper & Row: New York, 1987.

(28) Benson, S. W. *The Foundations of Chemical Kinetics*; McGraw-Hill Book Co., Inc.: New York, 1960.

(29) Frost, A. A.; Pearson, R. G. *Kinetics and Mechanism*, 2nd ed.; John Wiley & Sons Inc.: New York, 1961; p 114.

(30) Ostwald, W. *Z. Chem.* **1888**, 2, 127. Guggenheim, E. A. *Philos. Mag.* **1926**, *1*, 538. Sturtevant, J. M. *J. Am. Chem. Soc.* **1937**, *59*, 699.

(31) van't Hoff, J. H. *Études de dynamique chimique*; F. Muller and Co.: Amsterdam, The Netherlands, 1884; p 87.

(32) Letort, M. *J. Chim. Phys.* **1937**, *34*, 206; *Bull. Soc. Chim. Fr.* **1942**, *9*, 1.

(33) Stewart, R. *The Proton: Applications to Organic Chemistry*; *Academic Press*: Orlando, FL, 1985. Klumpp, G. W. *Reactivity in Organic Chemistry*; Wiley-Interscience: New York, 1982.

(34) Klumpp, G. W. *Reactivity in Organic Chemistry*; Wiley-Interscience: New York, 1985.

(35) Lundberg, R. D.; Phillips, R. R.; Peiffer, D. G. *J. Polym. Sci., Part B: Polym. Phys.* **1989**, *27* (2), 245. Lundberg, R. D.; Phillips, R. R.; Peiffer, D. G. *Polym. Mater. Sci. Eng.* **1988**, *58*, 1064.